# Genome-wide association studies of global *Mycobacterium tuberculosis* resistance to thirteen antimicrobials in 10,228 genomes

The CRyPTIC Consortium[1]

## Abstract

The emergence of drug resistant tuberculosis is a major global public health concern that threatens the ability to control the disease. Whole genome sequencing as a tool to rapidly diagnose resistant infections can transform patient treatment and clinical practice. While resistance mechanisms are well understood for some drugs, there are likely many mechanisms yet to be uncovered, particularly for new and repurposed drugs. We sequenced 10,228 *Mycobacterium tuberculosis* (MTB) isolates worldwide and determined the minimum inhibitory concentration (MIC) on a grid of twofold concentration dilutions for 13 antimicrobials using quantitative microtiter plate assays. We performed oligopeptide- and oligonucleotide-based genome-wide association studies using linear mixed models to discover resistance-conferring mechanisms not currently catalogued. Use of MIC over binary resistance phenotypes increased heritability for the new and repurposed drugs by 26-37%, increasing our ability to detect novel associations. For all drugs, we discovered uncatalogued variants associated with MIC, including in the *Rv1218c* promoter binding site of the transcriptional repressor *Rv1219c* (isoniazid), upstream of the *vapBC20* operon that cleaves 23S rRNA (linezolid) and in the region encoding an α-helix lining the active site of Cyp142 (clofazimine, all $p<10^{-7.7}$). We observed that artefactual signals of cross resistance could be unravelled based on the relative effect size on MIC. Our study demonstrates the ability of very large-scale studies to substantially improve our knowledge of genetic variants associated with antimicrobial resistance in *M. tuberculosis*.

[1] For a list of all members of the CRyPTIC Consortium please see the section at the end of this manuscript.

# Introduction

Tuberculosis (TB) continues to represent a major threat to global public health, with the World Health Organization (WHO) estimating 10 million cases and 1.4 million deaths in 2019 alone [1]. Multidrug resistance (MDR) poses a major challenge to tackling TB; it is estimated that there were 465,000 cases of rifampicin resistant TB in 2019, of which 78% were resistant to the first-line drugs rifampicin and isoniazid – called MDR-TB [1]. While treatment is 85% successful overall, that drops to 57% for rifampicin-resistant and MDR-TB [1]; underdiagnosis and treatment failures then amplify the problem by encouraging onward transmission of MDR-TB [2]. New treatment regimens for MDR-TB are therefore an important focus, introducing new and repurposed drugs such as bedaquiline, clofazimine, delamanid and linezolid [3,4]; however resistance is already emerging [5,6,7].

Understanding mechanisms of resistance in TB is important for developing rapid susceptibility tests that improve individual patient treatment, recommending drug regimens that reduce the development of MDR and developing new and improved drugs that expand treatment options [8,9]. Genomics can accelerate drug susceptibility testing, replacing slower culture-based methods by predicting resistance from the sequenced genome rather than directly phenotyping the bacteria [10]. Genome sequencing-based susceptibility testing for first-line drugs has achieved sensitivities of 91.3-97.5% and specificities of 93.6-99.0% [11], surpassing the thresholds for clinical accreditation, motivating its adoption by multiple public health authorities [12]. In low-resource settings, molecular tests such as Cepheid GeneXpert® and other line probe assays offer rapid and more economical susceptibility testing by genotyping a panel of known resistance-conferring genetic variants [13], with performance close to that achieved by whole genome sequencing [14,15]. However, the

limited number of resistance-conferring mutations that can be included in such tests can lead to missed MDR diagnoses and incorrect treatment [11,16]. Both approaches rely on the development and maintenance of resistance catalogues of genetic variants [17,11].

In the discovery of resistance-conferring variants, traditional molecular approaches have been replaced by high-throughput, large-scale whole genome sequencing studies of hundreds to thousands of resistant and susceptible clinical isolates [18,19,20,21,22,23]. Despite the strong performance of genome-based resistance prediction for first-line drugs, knowledge gaps remain, especially for second-line drugs [24,25,17]. There are numerous challenges in the pursuit of previously uncatalogued resistance mechanisms. Very large sample sizes are needed to identify rarer resistance mechanisms with confidence. The lack of recombination in *Mycobacterium tuberculosis* makes it difficult to pinpoint resistance variants unless they arise on multiple genetic backgrounds, reiterating the need for large sample sizes. Sophisticated analyses are required that attempt to disentangle genetic causation from correlation [26]. A reliance on a binary resistance/sensitivity classification paradigm has hindered reproducibility for some drugs, by failing to mirror the continuous nature of resistance [27,28,29].

The aim of *Comprehensive Resistance Prediction for Tuberculosis: an International Consortium* (*CRyPTIC*) was to address these challenges by assembling a global collection of over 10,000 *M. tuberculosis* isolates from 27 countries followed by whole-genome sequencing and semi-quantitative determination of minimum inhibitory concentration (MIC) to 13 first- and second-line drugs using a bespoke 96-well broth micodilution plate assay. The development of novel, inexpensive, high-throughput drug susceptibility testing

assays allowed us to conduct the project at scale, while investigating MIC on a grid of twofold concentration dilutions [30,31]. Here we report the identification of previously uncatalogued resistance-conferring variants through 13 genome-wide association studies (GWAS) investigating MIC values in 10,228 *M. tuberculosis* isolates. We employed a linear mixed model (LMM) to identify putative causal variants while controlling for confounding and genome-wide linkage disequilibrium (LD). We developed a novel approach to testing associations at both 10,510,261 oligopeptides (11-mers) and 5,530,210 oligonucleotides (31-mers) to detect relevant genetic variation in both coding and non-coding sequences, and to avoid a reference-based mapping approach that can inadvertently miss significant variation. We report previously uncatalogued variants associated with MIC for all 13 drugs, focusing on variants in the 20 most significant genes per drug. We highlight notable discoveries for each drug, and demonstrate the ability of large-scale studies to improve our knowledge of genetic variants associated with antimicrobial resistance in *M. tuberculosis*.

# Results

CRyPTIC collected isolates from 27 countries worldwide, oversampling for drug resistance [31]. 10,228 genomes were included in total across the GWAS analyses; 533 were lineage 1, 3581 lineage 2, 805 lineage 3, and 5309 lineage 4. Due to rigorous quality control, we dropped samples for each drug as detailed in the methods, resulting in a range of 6,388-9,418 genomes used in each GWAS (**Figure 1**). Minimum inhibitory concentrations (MICs) were determined on a grid of twofold concentration dilutions for 13 antimicrobials using quantitative microtiter plate assays: first-line drugs ethambutol, isoniazid and rifampicin; second-line drugs amikacin, ethionamide, kanamycin, levofloxacin, moxifloxacin and rifabutin and the new and repurposed drugs bedaquiline, clofazimine, delamanid and linezolid. The phenotype distributions differed between the drugs, with low numbers of sampled resistant isolates for the new and repurposed drugs which have not yet been widely used in tuberculosis treatment (**Figure 1**, **Supplementary Figure 1**). Assuming $\log_2$ MIC epidemiological cut-offs (ECOFFs) of 0.25 (bedaquiline, clofazimine), 0.12 (delamanid) and 1 mg/L (linezolid) [31], the GWAS featured 66 isolates resistant to bedaquiline, 97 resistant to clofazimine, 77 resistant to delamanid and 67 resistant to linezolid. We performed oligopeptide- and oligonucleotide-based GWAS analyses, controlling for population structure using linear mixed models (LMMs). We focused initially on oligopeptides, interpreting oligonucleotides only where necessary for clarifying results.

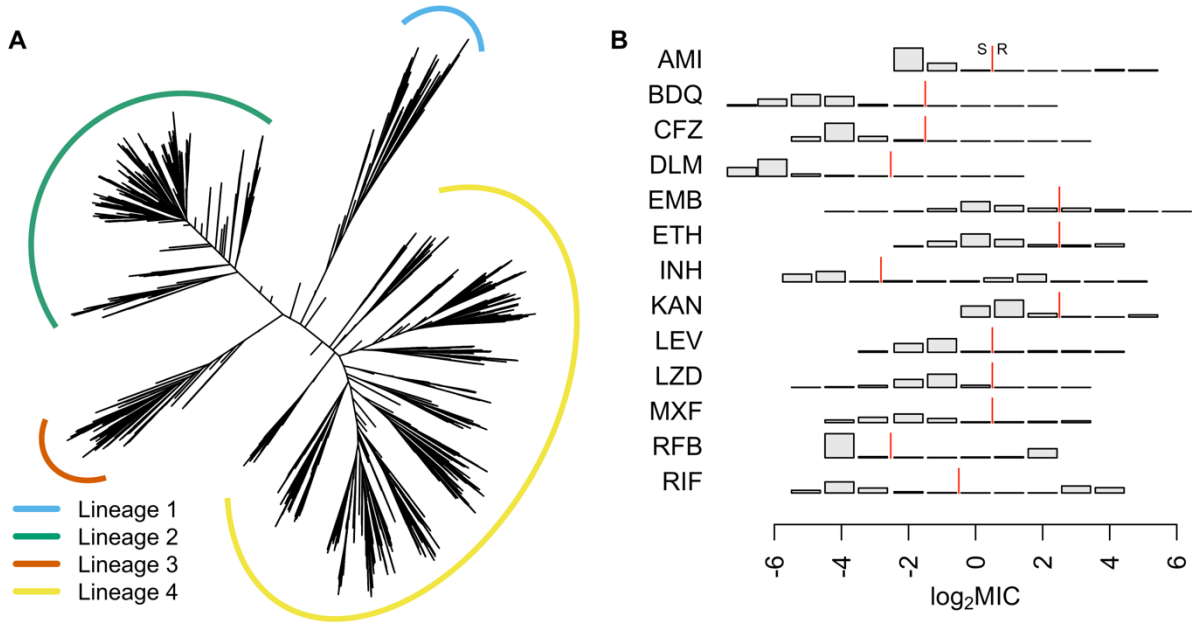


**Figure 1 A** Phylogeny of 10,228 isolates sampled globally by CRyPTIC used in the GWAS analyses. Lineages are coloured yellow (lineage 1), green (2), blue (3) and orange (4). Branch lengths have been square root transformed to visualise the detail at the tips. **B** Distributions of the $\log_2$ MIC measurements for all 13 drugs in the GWAS analyses, amikacin (AM), bedaquiline (BDQ), clofazimine (CFZ), delamanid (DLM), ethambutol (EMB), ethionamide (ETH), isoniazid (INH), kanamycin (KAN), levofloxacin (LEV), linezolid (LZD), moxifloxacin (MXF), rifabutin (RFB) and rifampicin (RIF). The red line indicates the ECOFF breakpoint for binary resistance versus sensitivity calls [31].

Estimates of sample heritability (variance in the phenotype explained by additive genetic effects) were higher for MIC compared to binary resistant vs. sensitive phenotypes for the new and repurposed drugs bedaquiline, clofazimine, delamanid and linezolid by at least 26%. Across drugs, binary heritability ranged from 0-94.7% and MIC heritability from 36.0-95.6%, focusing on oligopeptides (**Figure 2, Supplementary Figure 2 and Supplementary Table 1**). For delamanid, binary heritability was not significantly different from zero ($2.99\times10^{-6}$; 95% confidence interval (CI) 0.0-0.5%), while MIC heritability was 36.0% (95% CI

124 28.9-43.1%). Heritability estimates were more similar between binary and MIC phenotypes
125 for the remaining drugs, differing by -3.6 to +5.2%.
126

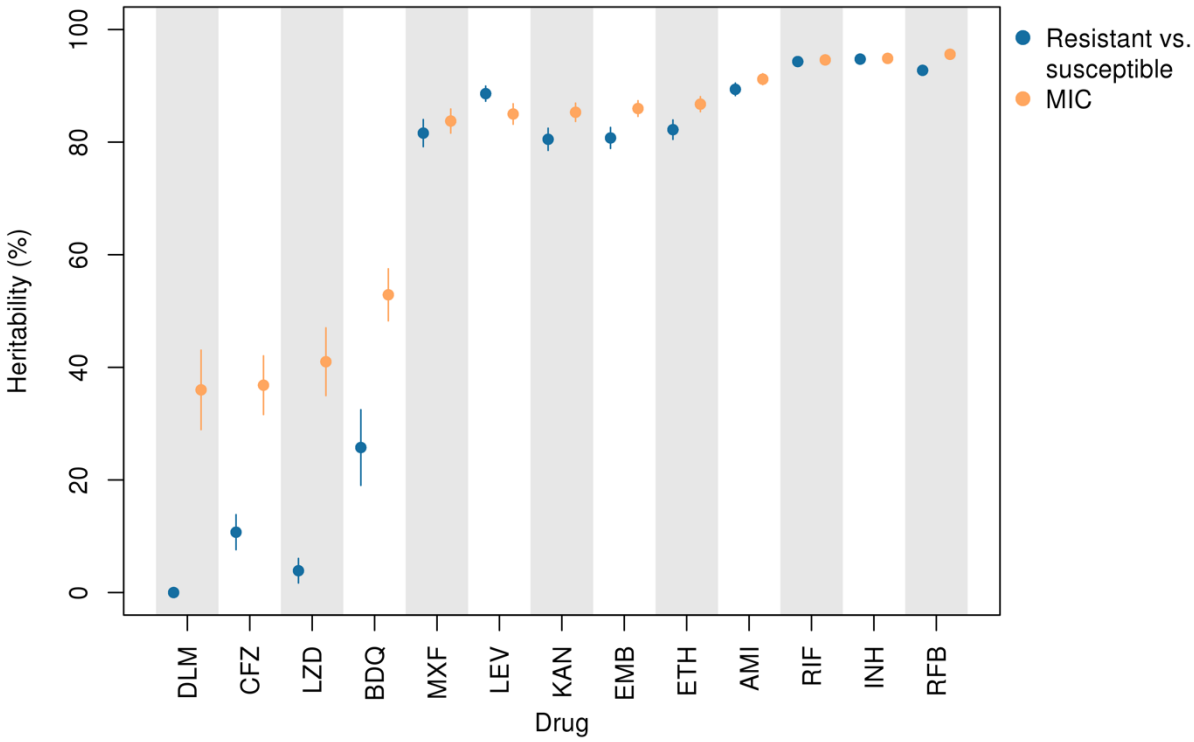


127

128 **Figure 2** MIC heritability (orange) versus binary (resistant/sensitive) heritability (blue) assuming additive
129 genetic variation in oligopeptide presence/absence across 13 drugs, DLM (delamanid), clofazimine (CFZ),
130 linezolid (LZD), bedaquiline (BDQ), moxifloxacin (MXF), levofloxacin (LEV), kanamycin (KAN), ethambutol
131 (EMB), ethionamide (ETH), amikacin (AM), rifampicin (RIF), isoniazid (INH), rifabutin (RFB). Lines depict 95%
132 confidence intervals. MIC heritability was at least 26% higher than binary heritability for the new and
133 repurposed drugs bedaquiline, clofazimine, delamanid and linezolid.

134

135 GWAS identified oligopeptide variants associated with changes in MIC for all 13 drugs after
136 controlling for population structure (**Figure 3**, **Table 1**, **Supplementary Figure 3-4**). In total,
137 across the drugs, we tested for associations at 10,510,261 variably present oligopeptides
138 and 5,530,210 oligonucleotides; these captured substitutions, insertions and deletions. The

drugs differed in the number of genes or intergenic regions that were significant, the drugs with fewest significant genes being isoniazid (12), levofloxacin (13) and moxifloxacin (6). We defined the significance of a gene or intergenic region by the most significant oligopeptide within it, and assessed all significant variants above a 0.1% minor allele frequency (MAF) threshold for the top 20 significant genes. The top 20 genes for each drug are detailed in **Table 1**. Some variants were identified in novel genes, some were novel variants in known genes, and some were known variants. We highlight examples of these (in reverse order) in the following sections. Highlighted examples have been chosen to exclude genes or variants in LD with other regions where possible; some are in LD with other less significant variants.

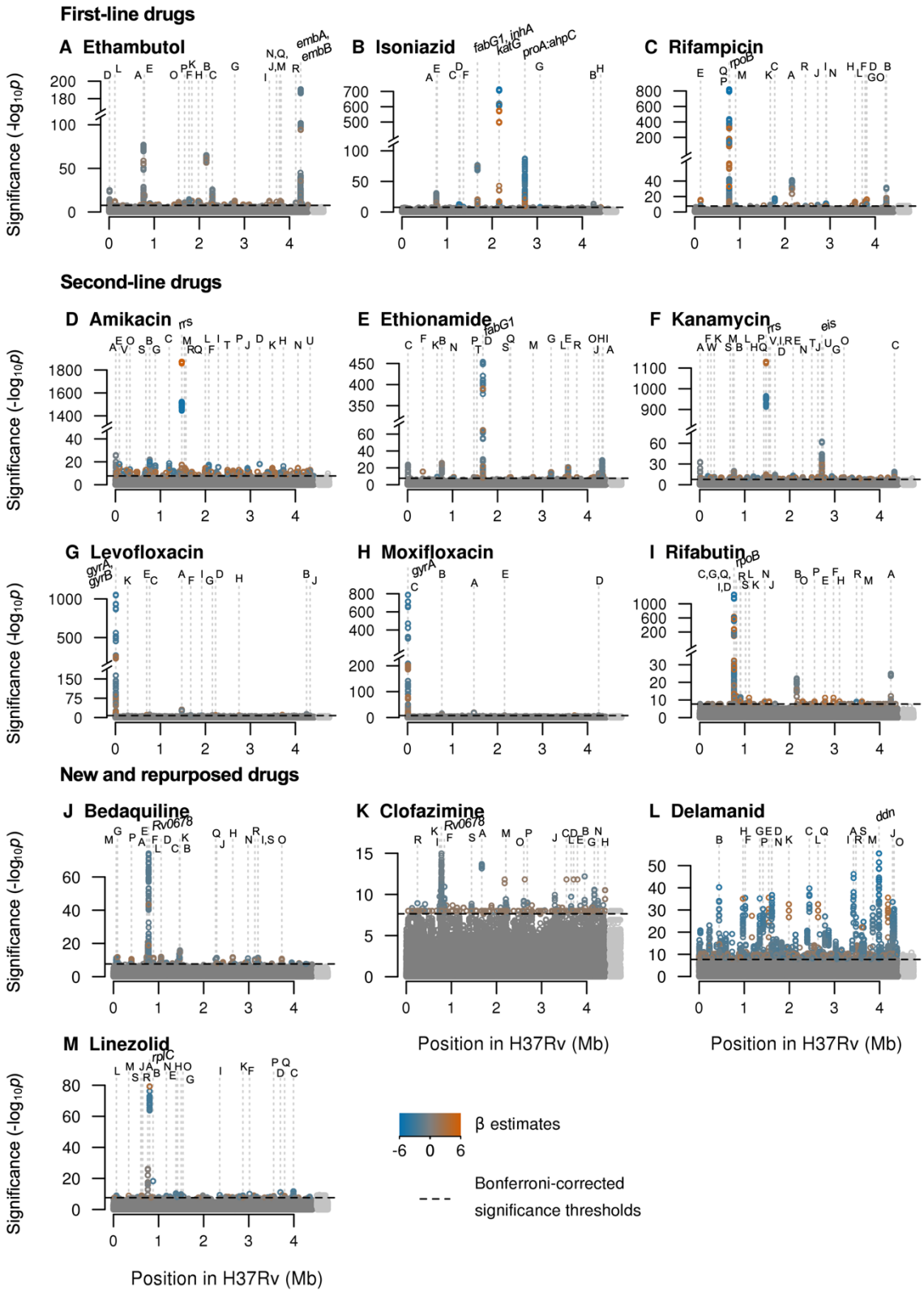


**Figure 3** Manhattan plots of regions containing oligopeptide variants associated with MIC across 13 drugs. Significant oligopeptides are coloured by the direction (orange=increase, blue=decrease) and magnitude of their effect size on MIC, estimated by LMM [32]. Bonferroni-corrected significance thresholds are shown by

the black dashed lines. The top 20 genes ranked by their most significant oligopeptides are annotated alphabetically. Gene names separated by colons indicate intergenic regions. Gene names for those annotated with letters can be found in Table 1. Oligopeptides were aligned to the H37Rv reference; unaligned oligopeptides are plotted to the right in light grey.

We assessed whether the top genes for each drug were in either of two previously described resistance catalogues [17,11]; we describe variants not in these catalogues as uncatalogued (**Table 1**). The interpretation of oligopeptides and oligonucleotides required manual curation to determine the underlying variants they tagged, and the most significant oligopeptide or oligonucleotide for each allele captured by the significant signals are described in **Supplementary table 2** and the **Supplementary text**. For 8/13 drugs with previously catalogued resistance determinants, the most significant GWAS signal in CRyPTIC was a previously catalogued variant, consistent with previous GWAS [18,19,20,21,22,23]. The most significant catalogued variants for each drug were (lowercase for nucleotides, uppercase for amino acids): *rrs* a1401g (amikacin, kanamycin), *embB* M306V (ethambutol), *fabG1* c−15t (ethionamide), *katG* S315T (isoniazid), *gyrA* D94G (levofloxacin, moxifloxacin), and *rpoB* S450L (rifampicin) [17,11]. For the remaining drugs with no previously catalogued resistance determinants, the genes identified by the top signals were: *Rv0678* (bedaquiline, clofazimine), *ddn* (delamanid), *fabG1* (ethionamide), *katG* (isoniazid), *rplC* (linezolid) and *rpoB* (rifabutin). The top variants identified for each drug were all significant at $p<1.04\text{x}10^{-15}$.

For many drugs, the direction of effect of the most significant oligopeptide variants was to decrease MIC (**Supplementary Figure 5**), implying that low-MIC oligopeptides and oligonucleotides are more likely to be genetically identical across strains than high-MIC

177 haplotypes. This would be consistent with the independent evolution of increased MIC from
178 a shared, low-MIC TB ancestor. Uncatalogued variants significantly associated with MIC are
179 important because they could improve resistance prediction and shed light on underlying
180 resistance mechanisms; they may be novel or previously implicated in resistance but not to
181 a standard of evidence sufficient to be catalogued. We discuss the choice of catalogues in
182 the Discussion [17,11].
183

184

| Drug | Top significant genes and intergenic regions |
|---|---|
| **First-line** | |
| **Ethambutol** | ***embB***, *rpoB* (A), *katG* (B), ***embA***, *pncA* (C), *gyrA* (D), *rpsL* (E), *Rv1565c* (F), *Rv2478c:Rv2481c* (G), *Rv1752* (H), *Rv3183:Rv3188*$^{R}$ (I), *dxs2:Rv3382c*$^{R}$ (J), *rpsA/coaE* (K), *ctpI* (L), *guaA* (M), *moaC3:Rv3327*$^{R}$ (N), *lprF:Rv1371*$^{R}$ (O), *fabG1* (P), *spoU* (Q), *glpK* (R) |
| **Isoniazid** | ***katG***, ***proA:ahpC***, ***fabG1***, *rpoB* (A), ***inhA***, *embB* (B), *Rv1139c:Rv1140* (C), *Rv1158c* (D), *rpsL* (E), *Rv1219c* (F), *ftsK/Rv2749* (G), *gid* (H) |
| **Rifampicin** | ***rpoB***, *katG* (A), *embB* (B), *Rv1565c* (C), *guaA* (D), *ctpI* (E), *spoU* (F), *dxs2:Rv3382c*$^{R}$ (G), *Rv3183:Rv3188*$^{R}$ (H), *relA* (I), *proA:ahpC* (J), *fabG1* (K), *moaC3:Rv3327*$^{R}$ (L), *Rv0810c* (M), *fadD9* (N), *Rv3779* (O), *rpsL* (P), *rpoC* (Q), *Rv2190c:Rv2191* (R) |
| **Second-line** | |
| **Amikacin** | ***rrs***, *gyrA* (A), *rpoB* (B), *echA8* (C), *Rv2896c* (D), *Rv0078A* (E), *Rv1830* (F), *Rv0792c/Rv0793* (G), *PPE54* (H), *Rv2041c* (I), *PPE42* (J), *cyp141:Rv3122* (K), *Rv1765c*$^{R}$ (L), *lprF:Rv1371*$^{R}$ (M), *espA:ephA* (N), *narU* (O), *rne* (P), *Rv1393c* (Q), *Rv1362c* (R), *Rv0579* (S), *glnE* (T), *ethA* (U), *Rv0208c:Rv0209* (V) |
| **Ethionamide** | ***fabG1***, *ethA* (A), *rpoB* (B), *gyrA* (C), *inhA* (D), *whiB7* (E), *PPE3* (F), *mpt53* (G), *embB* (H), *eccA1* (I), *embA* (J), *Rv0565c* (K), *fadB4* (L), *plsC* (M), *Rv0920c* (N), *Rv3698* (O), *rrs* (P), *pncA* (Q), *PPE56* (R), *Rv2019* (S), *lprF:Rv1371*$^{R}$ (T) |
| **Kanamycin** | ***rrs***, ***eis***, *gyrA* (A), *rpoB* (B), *ethA* (C), *fabG1* (D), *Rv1830* (E), *ptbB* (F), *PPE42* (G), *echA8* (H), *lprF:Rv1371*$^{R}$ (I), *Rv2348c:plcC* (J), *narU* (K), *pgi* (L), *mmaA4* (M), *pncA* (N), *viuB* (O), *lprC* (P), *murA* (Q), *Rv1393c* (R), *Rv0579* (S), *glnE* (T), *rne* (U), *Rv1362c* (V), *Rv0208c:Rv0209* (W) |
| **Levofloxacin** | ***gyrA***, *rrs* (A), ***gyrB***, *embB* (B), *rpoB* (C), *vapC36* (D), *mce2F* (E), *fabG1* (F), *katG* (G), *folC* (H), *tlyA* (I), *ethA* (J), *Rv0228* (K) |
| **Moxifloxacin** | ***gyrA***, *rrs* (A), *rpoB* (B), *gyrB* (C), *embB* (D), *katG* (E) |
| **Rifabutin** | *rpoB*, *embB* (A), *katG* (B), *rpoC* (C), *Rv0810c* (D), *Rv2478c:Rv2481c*$^{R}$ (E), *Rv2647:Rv2650c*$^{R}$ (F), *rplP* (G), *Rv2797c* (H), *cpsY* (I), *lysA* (J), *mprB* (K), *mprA* (L), *Rv3228* (M), *Rv1290c* (N), *pncA* (O), *Rv2277c:pitB*$^{R}$ (P), *Rv0726c* (Q), *cysA3/cysA2* (R), *Rv0914c* (S) |
| **New and repurposed** | |
| **Bedaquiline** | *Rv0678*, *rpoB* (A), *rrs* (B), *atpE* (C), *pgi* (D), *mmaA4* (E), *rplC* (F), *Rv0078A* (G), *era/amiA2* (H), *viuB* (I), *pncA* (J), *murA* (K), *Rv0792c/Rv0793* (L), *dnaB* (M), *Rv2665:clpC2* (N), *PPE54* (O), *Rv0332* (P), *Rv2019* (Q), *vapC22* (R), *Rv2896c* (S) |
| **Clofazimine** | *Rv0678*, *fabG1* (A), *cyp142* (B), *Rv3183:Rv3188*$^{R}$ (C), *moaC3:Rv3327*$^{R}$ (D), *dxs2:Rv3382c*$^{R}$ (E), *mmsA* (F), *Rv3723:Rv3725* (G), *gid* (H), *rpoB* (I), *pks1* (J), *mmaA2:mmaA1* (K), *Rv3273* (L), *mce3R/yrbE3A* (M), *Rv3796* (N), *mez* (O), *Rv2390c* (P), *yrbE3B* (Q), *Rv0207c* (R), *argS* (S) |
| **Delamanid** | *ddn*, *fadE22* (A), *fba* (B), *Rv2180c* (C), *gap* (D), *lprF:Rv1371*$^{R}$ (E), *Rv0914c* (F), *Rv1200* (G), *fadE10* (H), *dinP* (I), *mmpL8* (J), *cut1*$^{R}$ (K), *PPE39*$^{R}$ (L), *Rv3430a:gadB* (M), *Rv1429* (N), *Rv3847* (O), *pknH* (P), *plsC* (Q), *agpS* (R), *Rv3263* (S) |
| **Linezolid** | *rplC*, *rpoB* (A), *emrB* (B), *Rv3552* (C), *add* (D), *vapC33* (E), *ppgK* (F), *pncB1:Rv1331* (G), *lprA* (H), *pafA* (I), *PE_PGRS6* (J), *vapB20* (K), *Rv0061c* (L), *PE_PGRS4* (M), *Rv1049* (N), *lprF:Rv1371*$^{R}$ (O), *Rv3183:Rv3188*$^{R}$ (P), *dxs2:Rv3382c*$^{R}$ (Q), *Rv0556* (R), *Rv0514* (S) |

185 **Table 1** The top genes or intergenic regions ranked by their most significant oligopeptides per drug**,** up to a

186 maximum of 20 (more only when the 20$^{th}$ was tied). Genes are highlighted in bold if they were catalogued for

187 that drug by [17,11]. Gene names separated by colons indicate intergenic regions. Genes or intergenic regions

188 capturing repeat regions are highlighted with the superscript $^{R}$. Alphabetic characters following gene names
189 are used to cross-reference with the corresponding Manhattan plots in Figure 3.

190

191 We next looked at uncatalogued variants in known resistance-conferring genes. We
192 identified uncatalogued variants in *gyrB* associated with levofloxacin and moxifloxacin MIC
193 (minimum *p*-value levofloxacin: $p<10^{-15.6}$, moxifloxacin: $p<10^{-11.6}$. The primary mechanisms
194 of resistance to the fluoroquinolones levofloxacin and moxifloxacin are mutations in *gyrA* or
195 *gyrB*, the subunits of DNA gyrase. The *gyrB* Manhattan plots for levofloxacin and
196 moxifloxacin both contained two adjacent peaks within the gene, but for each drug just one
197 of the two peaks was significant, and these differed between the drugs (**Figure 4**).
198 Interpretation of oligopeptides and oligonucleotides requires an understanding of the
199 variants that they capture, which we visualised by aligning them to H37Rv and interpreting
200 the variable sites (e.g. **Figure 4C-D**). For levofloxacin the peak centred around amino acid
201 461. Significant oligopeptides captured amino acids 461 and 457, which are both
202 uncatalogued [17,11] with 457 falling just outside of the *gyrB* quinolone resistance-
203 determining region (QRDR-B) [33]. Oligopeptides capturing 461N were associated with
204 increased MIC (e.g. **N**SAGGSAKSGR, $-\log_{10}p$ = 15.65, effect size $\beta$ = 2.46, present in 15/7300
205 genomes). Oligopeptides capturing the reference alleles at codons 461 and 457 were
206 significantly associated with lower MIC (e.g. 461D: **D**SAGGSAKSGR, $-\log_{10}p$ = 13.47, $\beta$ = -2.14,
207 present in 7278/7300 genomes; 457V/461D: SELY**V**VEG**D**SA, $-\log_{10}p$ = 12.51, $\beta$ = -1.96,
208 present in 7272/7300 genomes). For moxifloxacin, the peak centred around amino acid 501.
209 Significant oligopeptides captured amino acids 499 and 501. Oligopeptides capturing 501D
210 were associated with increased MIC (e.g. NT**D**VQAIITAL, $-\log_{10}p$ = 10.64, $\beta$ = 1.86, present in
211 23/6388 genomes). Oligopeptides capturing the reference allele at codons 499 and 501

were associated with lower MIC (e.g. **NTE**VQAIITAL, -$\log_{10}p$ = 11.63, $\beta$ = -1.33, present in 6332/6388 genomes). Amino acids 461 and 501 are at the interface between *gyrB* and the bound fluroquinolone [34]. *gyrB* is included in the reference catalogues for predicting levofloxacin but not moxifloxacin resistance, therefore our results support inclusion in future moxifloxacin catalogues [17,11].

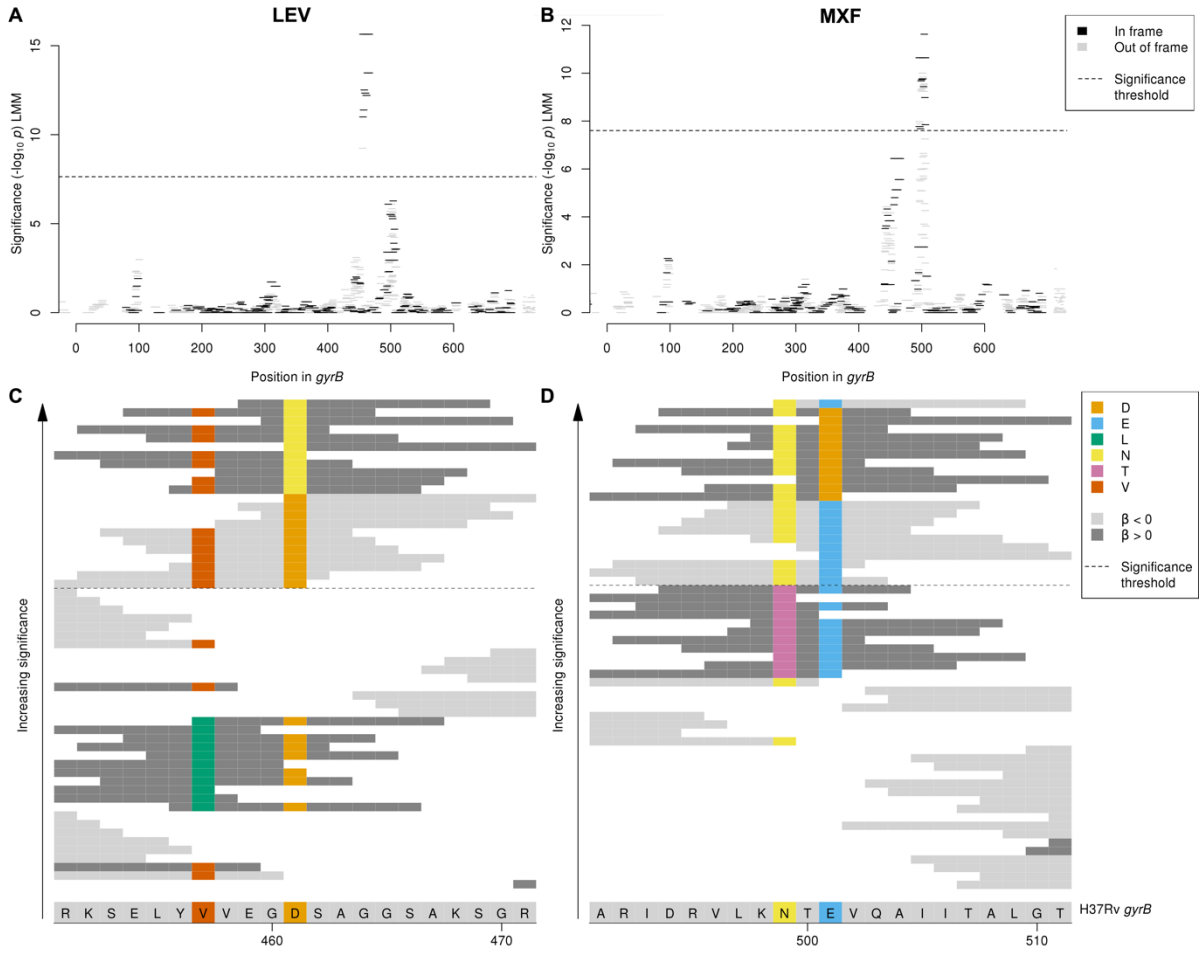


**Figure 4** Interpreting significant oligopeptide variants for levofloxacin and moxifloxacin MIC in *gyrB***.** Oligopeptide Manhattan plots are shown for **A** levofloxacin **B** moxifloxacin. Oligopeptides are coloured by the reading frame that they align to, black for in frame and grey for out of frame in *gyrB*. Oligopeptides aligned to the region by nucmer but not realigned by BLAST are shown in grey on the right hand side of the plots. The black dashed lines indicate the Bonferroni-corrected significance thresholds – all oligopeptides above the line are genome-wide significant. Alignment is shown of oligopeptides significantly associated with **C** levofloxacin

and **D** moxifloxacin. The H37Rv reference codons are shown at the bottom of the figure, grey for an invariant site, coloured at variant site positions. The background colour of the oligopeptides represents the direction of the β estimate, light grey when $\beta < 0$ (associated with lower MIC), dark grey when $\beta > 0$ (associated with higher MIC). Oligopeptides are coloured by their amino acid residue at variant positions only.

Next we looked at specific examples of significant associations identified by GWAS in genes not catalogued by [17,11] for each of the drugs. A well-recognized challenge in GWAS for antimicrobial resistance is the presence of artefactual cross resistance. To mitigate this risk, we preferentially highlight variants significantly associated with a single drug. However, many catalogued resistance variants demonstrated artefactual cross resistance. For example, variants in the rifampicin resistance determining region were in the top 20 significant associations for all drugs except for delamanid (**Table 1**). Interestingly, we observed that the magnitude of effect sizes was often larger on MIC of the drug to which catalogued variants truly confer resistance (**Supplementary Figure 6**). For example, the effect sizes for significant oligopeptides in *rpoB* were greater for rifampicin and rifabutin than for all other drugs. This suggests that the β estimates could help to prioritise drugs for follow up when genes are significantly associated with multiple drugs.

**First-line drugs**

**Ethambutol and rifampicin.** Oligonucleotides downstream of *spoU* (*Rv3366*) were significantly associated with ethambutol and rifampicin MIC (minimum *p*-value $p<10^{-10.0}$, **Supplementary Figure 7**). SpoU is a tRNA/rRNA methylase, shown to have DNA methylation activity [35]. As the association was outside of the coding region, we interpreted oligonucleotides for this association. Oligonucleotides associated with increased MIC

249 captured the relatively common adenine 20 nucleotides downstream of the stop codon (e.g.
250 C**A**AACCAGCCGGTATGCGCACAACGAAGCTC, RIF: -$\log_{10}p$ = 12.82, $\beta$ = 3.19, present in
251 159/8394 genomes; EMB: -$\log_{10}p$ = 10.86, $\beta$ = 1.36, present in 163/7081 genomes). This
252 mutation has been identified in previous association studies as associated with rifampicin
253 and ethambutol resistance [36,37] but has not been catalogued. The new evidence provided
254 by CRyPTIC supports re-evaluation of this putative resistance-conferring variant. The
255 simultaneous association of *spoU* with rifampicin and ethambutol may be an example of
256 artefactual cross resistance. The effect sizes on MIC for rifampicin ($\beta$ = 3.19) were larger
257 than for ethambutol ($\beta$ = 1.36), suggesting prioritisation of the rifampicin association over
258 the ethambutol association reported here.
259
260 **Isoniazid.** Oligopeptides in *Rv1219c* were significantly associated with isoniazid MIC
261 (minimum *p*-value $p<10^{-8.5}$, **Supplementary Figure 8**). Rv1219c represses transcription of the
262 Rv1217c-Rv1218c multidrug efflux transport system [38]. It binds two motifs, a high-affinity
263 intergenic sequence in the operon's promoter, and a low-affinity intergenic sequence
264 immediately upstream of *Rv1218c* [38]. The peak signal of association coincides with the C-
265 terminal amino acids 188-189 in the low-affinity binding domain of Rv1219c. Multiple
266 extremely low frequency oligopeptides were associated with increased MIC, present in just
267 one or two genomes. In contrast, oligopeptides containing the reference alleles at codons
268 188-189 were present in 8919/8929 genomes and strongly associated with decreased MIC
269 (e.g. EVYT**EG**LLADR, -$\log_{10}p$ = 8.46, $\beta$ = -3.63, present in 8919/8929 genomes). Substitutions
270 at these positions may therefore derepress the multidrug efflux transport system. Indeed,
271 overexpression of Rv1218c has been observed to correlate with higher isoniazid MIC in vitro
272 [39].

## Second-line drugs

**Amikacin and kanamycin.** Oligopeptides in *PPE42* (*Rv2608*) were significantly associated with aminoglycoside MIC, for both amikacin and kanamycin (minimum *p*-value $p<10^{-12.8}$, **Supplementary Figure 9**). PPE42 is an outer membrane-associated PPE-motif family protein and potential B cell antigen. It elicits a high humoral and low T cell response [40] and is one of four antigens in the vaccine candidate ID93 [41]. The C-terminal major polymorphic tandem repeats (MPTRs) contain a region of high antigenicity [40]. The peak association with MIC occurred halfway along the coding sequence. The oligopeptides most associated with higher MIC captured a premature stop codon at position 290 (e.g. PLLE*****AARFIT, amikacin $-\log_{10}p = 11.25$, $\beta = 3.12$, present in 38/8430 genomes; kanamycin $-\log_{10}p = 10.25$, $\beta = 2.33$, present in 40/8748 genomes). A nearby premature stop codon at amino acid 484 was previously identified in a multi-drug resistant strain [42], supporting the proposition that truncation of PPE42 enhances aminoglycoside resistance.

**Ethionamide.** Oligopeptides and oligonucleotides upstream and within the transcriptional regulator *whiB7* (*Rv3197A*) were significantly associated with ethionamide MIC (minimum *p*-value $p<10^{-18.2}$, **Supplementary Figure 10**). Oligonucleotides associated with higher MIC captured a single-base guanine deletion 177 bases upstream of *whiB7*, within the 5' untranslated region [43] (e.g. AACCGTGTCGCCGCCGCGACTGACGAGTCCT, $-\log_{10}p = 18.18$, $\beta = 2.16$, present in 46/8287 genomes), while oligopeptides associated with higher MIC captured multiple substitutions within the AT-hook motif known to bind AT-rich sequences [44,45] (e.g. DQGSIVSQQHP, $-\log_{10}p = 10.85$, $\beta = 1.96$, present in 22/8287 genomes). Substitutions in the AT-hook motif may disrupt the binding with the *whiB7* promoter

297 sequence, while deletions upstream of *whiB7* have been shown to result in overexpression
298 of WhiB7 [46]. WhiB7 is induced by antibiotic treatment and other stress conditions and
299 activates its own expression along with other drug resistance genes, for example *tap* and
300 *erm* [45]. Variants in and upstream of another *whiB*-like transcriptional regulator, *whiB6*,
301 were previously found to be associated with resistance to ethionamide [19,47],
302 capreomycin, amikacin, kanamycin and ethambutol [22,23]. WhiB7 has been implicated in
303 cross-resistance to multiple drugs, including macrolides, tetracyclines and aminoglycosides
304 [45,46], however activation of WhiB7 is not induced by all antibiotics, for instance isoniazid
305 [43]. Interestingly, oligopeptides and oligonucleotides in or upstream of *whiB7* were not
306 found to be significantly associated with any of the other 12 antimicrobials. This could
307 indicate yet another mechanism by which *whiB7* is involved in resistance to anti-
308 tuberculosis drugs.
309
310 **Levofloxacin**. Oligopeptides in *tlyA* (*Rv1694*) were significantly associated with MIC of the
311 fluoroquinolone levofloxacin (minimum *p*-value $p<10^{-7.8}$, **Supplementary Figure 11**). *tlyA*
312 encodes a methyltransferase which methylates ribosomal RNA. Variants in *tlyA*, including
313 loss-of-function mutations, confer resistance to the aminoglycosides viomycin and
314 capreomycin [48] by knocking out its methyltransferase activity [49].
315 An extremely low frequency oligopeptide was associated with increased MIC, and captured
316 a one-nucleotide adenosine insertion between positions 590 and 591 in codon 198 in a
317 conserved region [50]. In contrast, oligopeptides containing the reference alleles in this
318 region were associated with decreased MIC (e.g. GKGQVGPGGV**V**, $-\log_{10}p = 7.83$, $\beta = -1.86$,
319 present in 7281/7300 genomes). The resulting frameshift likely mimics the knockout effect
320 of deleting the 27 C-terminal residues of TlyA, which ablates methyltransferase activity [51].

While loss-of-function mutations conferring antimicrobial resistance were previously reported to specifically increase aminoglycoside MIC, fluoroquinolones were not investigated [52]. The signal in *tlyA* may therefore reveal genuine, previously unidentified cross-resistance.

**Rifabutin**. Oligonucleotides in *cysA2* (*Rv0815c*) and *cysA3* (*Rv3117*) were significantly associated with rifabutin MIC (minimum *p*-value $p<10^{-7.7}$, **Supplementary Figure 12**). They encode identical proteins, which are putative uncharacterised thiosulfate:cyanide sulfurtransferases, known as rhodaneses, belonging to the essential sulfur assimilation pathway, secreted during infection [53]. No genome-wide significant signals associated specific oligopeptides or oligonucleotides with higher MIC. Significant oligonucleotides that aligned to *cysA2* and *cysA3* were associated with lower MIC. They captured two variants: a synonymous nucleotide substitution, a thymine at position 117 in codon 39, and a non-synonymous nucleotide substitution, a guanine at position 103 inducing amino acid substitution 35D (e.g. CATAT**G**ACCGTGACCATAT**T**GCCGGCGCGAT, $-\log_{10}p = 7.74$, $\beta = -2.65$, present in 9396/9418 genomes). These positions coincide with the rhodanese characteristic signature in the N-terminal region, important for rhodanese stability [54]. However, the mechanism of resistance against rifabutin remains to be elucidated.

**New and repurposed drugs**

**Bedaquiline**. Oligonucleotides situated in the region of overlap at the 3' ends of *amiA2* (*Rv2363*) and *era* (*Rv2364c*) were significantly associated with bedaquiline MIC (minimum *p*-value $p<10^{-10.5}$, **Supplementary Figure 13**). These genes encode an amidase and a GTPase, respectively, on opposite strands. Of the two top oligonucleotides associated with higher

MIC, the first captures two substitutions that are synonymous in *era*, 7-19 nucleotides upstream of the stop codon, and 3' non-coding in *amiA2*, 4-16 nucleotides downstream of the stop codon (e.g. CCCCAAACAGCT**T**GGCCGACTGGG**G**TTTTAG, $-\log_{10}p = 10.47$, $\beta = 1.26$, present in 7919/8009 genomes). The second additionally captures a variant that induces a non-synonymous guanine substitution at position 1451 in *amiA2*, and is 3' intergenic in *era*, one nucleotide downstream of the stop codon (e.g. CAAACAGCT**T**GGCCGACTGGG**G**TTTTAG**C**TC, $-\log_{10}p = 7.87$, $\beta = 0.88$, present in 7898/8009 genomes). Interestingly, AmiA2 has previously been identified at lower abundance in MDR compared to sensitive isolates [55], and Era (but not AmiA2) has been shown to be required for optimal growth of H37Rv [56]. These variants may therefore enhance tolerance to bedaquiline.

**Clofazimine**. Oligopeptides in *cyp142* (*Rv3518c*), which encodes a cytochrome P450 enzyme with substrates of cholesterol/cholest-4-en-3-one, were significantly associated with clofazimine MIC (minimum *p*-value $p<10^{-12.2}$, **Supplementary Figure 14**). Oligopeptides associated with higher MIC captured the amino acid residue 176I (e.g. EDFQIT**I**DAFA, $-\log_{10}p = 7.99$, $\beta = 1.14$, present in 100/7297 genomes). The association signal falls within the F $\alpha$-helix of CYP142, which lines the entrance to the active site with largely hydrophobic residues, forming part of the substrate binding pocket [57,58]. Homology with CYP125 suggests that residue 176 captured by the GWAS is within 5 Å of the binding substrate [58]. The potential for cytochrome P450 enzymes as targets for anti-tuberculosis drugs has been highlighted [59]; CYP142 is inhibited by azole drugs [59] and has been found to form a tight complex with nitric oxide (NO) [60]. The anti-mycobacterial activity of clofazimine has been shown to produce reactive oxygen species [61], therefore the substitution identified by the

GWAS may disrupt the binding of NO to CYP142. Methionine and isoleucine are both hydrophobic residues, so the mechanism for how this would disrupt binding is unknown.

**Delamanid**. Oligonucleotides in *pknH* (*Rv1266c*), which encodes a serine/threonine-protein kinase, were significantly associated with delamanid MIC (minimum *p*-value $p<10^{-30.2}$, **Supplementary Figure 15**). Delamanid is a prodrug activated by deazaflavin-dependent nitroreductase which inhibits cell wall synthesis. PknH phosphorylates the adjacent gene product EmbR [62], enhancing its binding of the promoter regions of the *embCAB* operon [63]. Mutations in *embAB* are responsible for ethambutol resistance [64]. The peak GWAS signal localized to the C-terminal periplasmic domain of PknH [62]. Oligonucleotides below our MAF threshold captured extremely low frequency triplet deletions of either ACG at nucleotides 1645-7 or GAC at nucleotides 1644-6. In contrast, oligonucleotides containing the reference alleles in this region were associated with decreased MIC (e.g. CAAGACGGTCACCGTCACGAATAAGGCCAAG , $-\log_{10}p = 30.21$, $\beta = -3.29$, present in 7555/7564 genomes). These variants likely disrupt intramolecular disulphide binding linking the two highly conserved alpha helices that form the V-shaped cleft of the C-terminal sensor domain [65]. Since NO is released upon activation of DLM, and deletion of PknH alters sensitivity to nitrosative and oxidative stresses [66], these rare variants may alter tolerance to delamanid mediated by NO.

**Linezolid**. Oligonucleotides in *vapB20* (*Rv2550c*) were significantly associated with linezolid MIC (minimum *p*-value $p<10^{-8.6}$, **Supplementary Figure 16**). VapB20 is an antitoxin cotranscribed with its complementary toxin VapC20 [67]. The latter modifies 23S rRNA [68], the target of linezolid which inhibits protein synthesis by competitively binding 23S rRNA.

The peak signal in *vapB20* occurred just upstream of the promotor and VapB20 binding sites, 21 nucleotides upstream of the -35 region [68]. Oligonucleotides below our MAF threshold associated with increased MIC shared a cytosine 33 nucleotides upstream of *vapB20*, replacing the reference nucleotide thymine which was associated with decreased MIC (e.g. GAATCGG**A**TGCTTGCCGCTGGCTGCCGAGTT, $-\log_{10}p = 8.60$, $\beta = -2.02$, present in 6724/6732 genomes). This substitution may derepress the toxin, which could interrupt linezolid binding by cleaving the Sarcin-Ricin loop of 23S rRNA.

## Discussion

In this study we tested oligopeptides and oligonucleotides for association with quantitative MIC measurements for 13 antimicrobials to identify novel resistance determinants. Analysing MIC rather than binary resistance phenotypes enabled identification of variants that cause subtle changes in MIC. This is important, on the one hand, because higher rifampicin and isoniazid MIC in sensitive isolates are associated with increased risk of relapse after treatment [69]. Conversely, low-level resistance among isolates resistant to RIF and isoniazid mediated by particular mutations may sometimes be overcome by increasing the drug dose, or replacing rifampicin with rifabutin, rather than changing to less desirable drugs with worse side effects [70,71,72,73,74]. The investigation of MIC was particularly effective at increasing heritability for the new and repurposed drugs.

The MICs were positively correlated between many drugs, particularly amongst first-line drugs. Consequently, many of the 10,228 isolates we studied were MDR and XDR. In GWAS, this generates artefactual cross resistance, in which variants that cause resistance to one drug appear associated with other drugs to which they do not confer resistance. In practice,

it is difficult to distinguish between associations that are causal versus artefactual without experimental evidence. Nevertheless, we found frequent evidence of artefactual cross resistance: several genes and intergenic regions featured among the top 20 strongest signals of association to multiple drugs, including *rpoB* (12 drugs), *embB* (7), *fabG1* (7), *rrs* (6), *gyrA* (6), *katG* (6), *lprF:Rv1371* (6), *pncA* (5), *ethA* (4), *Rv3183:Rv3188* (4) *dxs2:Rv3382c* (4), *rpsL* (3) and *moaC3:Rv3327* (3). Among previously catalogued variants, we observed that the estimated effect sizes were usually larger in magnitude for significant true associations than significant artefactual associations (**Supplementary figure 4**). In future GWAS, this relationship could help tease apart true versus artefactual associations when a uncatalogued variant is associated with multiple drugs.

We focused on variants in the top twenty most significant genes identified by GWAS for each of the 13 drugs, classifying significant oligopeptides and oligonucleotides according to whether the variants they tagged were previously catalogued among known resistance determinants, or not. While the interpretation of oligopeptides and oligonucleotides required manual curation to determine the underlying variants they tagged, the approach had the advantage of avoiding reference-based variant calling which can miss important signals, particularly at difficult-to-map regions. For 8/13 drugs with previously catalogued resistance determinants, the most significant GWAS signal in CRyPTIC was a previously catalogued variant. Among the uncatalogued variants there are promising signals of association, including in the *Rv1218c* promoter binding site of the transcriptional repressor *Rv1219c* (associated with MIC for isoniazid) upstream of the *vapBC20* operon that cleaves 23S rRNA (linezolid) and in the region encoding a helix lining the active site of *cyp142* (clofazimine). These variants would benefit from further investigation via replication studies

441 in independent populations, experimental exploration of proposed resistance mechanisms,
442 or both.
443
444 We elected to classify significant variants as catalogued versus uncatalogued, rather than
445 known versus novel, for several reasons. The catalogues represent a concrete, pre-existing
446 knowledgebase collated by expert groups for use in a clinical context [17,11]. We chose
447 [17,11] as they are the most recent and up to date catalogues available for the drugs we
448 investigated. The inclusion criteria for variants to be considered catalogued are therefore
449 stringent; it follows that a class of variants exist that have been reported in the literature
450 but not assimilated into the catalogues [17,11]. The literature is vast and heterogenous,
451 with evidence originating from molecular, clinical and genome-wide association studies.
452 Inevitably, some uncatalogued variants in the literature will be false positives, while others
453 will be real but did not meet the standard of evidence or clinical relevance for cataloguing.
454 Evidence from CRyPTIC that supports uncatalogued variants in the latter group is of equal or
455 greater value than the discovery of completely novel variants, because it contributes to a
456 body of independent data supporting their involvement. For instance, *gyrB* did not appear
457 in the catalogues we used for moxifloxacin [17,11]. Yet our rediscovery of *gyrB* 501D
458 complements published reports associating the substitution with moxifloxacin resistance
459 [75,76,77], strongly enhancing the evidence in favour of inclusion in future catalogues.
460 Indeed, the recent WHO prediction catalogue, published after the completion of this study
461 and which draws on the CRyPTIC data analysed here includes the E501D resistance-
462 associated variant [78]. Moreover, of the five new genes added to the forthcoming WHO
463 catalogue [78] but not featuring in the catalogues [17,11] used here – *eis* (amikacin), *ethA*

464 (ethionamide), *inhA* (ethionamide), *rplC* (linezolid), *gyrB* (moxifloxacin) – we identify all as
465 containing significant variants by GWAS except one, *eis* (amikacin).
466
467 The combination of a very large dataset exceeding 10,000 isolates and quantification of
468 resistance via MIC enabled the CRyPTIC study to attribute a large proportion of fine-grained
469 variability in antimicrobial resistance in *M. tuberculosis* to genetic variation. Compared to a
470 parallel analysis of binary resistance phenotypes in the same samples, we observed an
471 increase in heritability of 26.1-37.1% for the new and repurposed drugs bedaquiline,
472 clofazimine, delamanid and linezolid. The improvement was most striking for delamanid,
473 whose heritability was not significantly different to zero for the binary resistance
474 phenotype. In contrast, the scope for improvement was marginal for the better-studied
475 drugs isoniazid and rifampicin, where MIC heritabilities of 94.6-94.9% were achieved. This
476 demonstrates the ability of additive genetic variation to explain almost all the phenotypic
477 variability in MIC for these drugs. Nevertheless, we were still able to find uncatalogued hits
478 for these drugs. The very large sample size also contributed to increased heritability
479 compared to previous pioneering studies. Compared to Farhat et al 2019 [22] who
480 estimated the heritability of MIC phenotypes in 1452 isolates, we observed increases in
481 heritability of 2.0% (kanamycin), 3.3% (amikacin), 14.0% (isoniazid), 10.8% (rifampicin),
482 11.2% (ethambutol) and 19.4% (moxifloxacin). Furthermore, many of the uncatalogued
483 signals we report here as significant detected rare variants at below 1% minor allele
484 frequency, underlining the ability of very large-scale studies to improve our understanding
485 of antimicrobial resistance not only quantitatively, but to tap otherwise unseen rare variants
486 that reveal new candidate resistance mechanisms.
487

# Materials and Methods

## Sampling frames

CRyPTIC collected isolates from 27 countries worldwide, oversampling for drug resistance, as described in detail in [31]. Clinical isolates were subcultured for 14 days before inoculation onto one of two CRyPTIC designed 96-well microtiter plates manufactured by ThermoFisher. The first plate used (termed UKMYC5) contained doubling-dilution ranges for 14 different antibiotics, the second (UKMYC6) removed para-aminosalicylic acid due to poor results on the plate [30] and changed the concentration of some drugs. Para-aminosalicylic acid was therefore not included in the GWAS analyses. Phenotype measurements were determined to be high quality, and included in the GWAS analyses, if three independent methods (Vizion, AMyGDA and BashTheBug) agreed on the value [31]. Sequencing pipelines differed slightly between the CRyPTIC sites, but all sequencing was performed using Illumina, providing an input of matched pair FASTQ files containing the short reads.

15,211 isolates were included in the initial CRyPTIC dataset with both genomes and phenotype measurements after passing genome quality control filters [31,79], however some plates were later removed due to problems identified at some laboratories with inoculating the plates [31]. Genomes were also excluded if they met any of the following criteria, determined by removing samples at the outliers of the distributions: (i) no high quality phenotypes for any drugs; (ii) total number of contigs > 3000; (iii) total bases in contigs $< 3.5\text{x}10^6$ or $> 5\text{x}10^6$; (iv) number of unique oligonucleotides $< 3.5\text{x}10^6$ or $> 5\text{x}10^6$; (v) sequencing read length not 150/151 bases long. This gave a GWAS dataset of 10,422 genomes used to create the variant presence/absence matrices. We used Mykrobe

512 [80,79,81] to identify *Mycobacterium* genomes not belonging to lineages 1-4 or
513 representing mixtures of lineages. This led to the exclusion of 193 genomes, which were
514 removed from GWAS by setting the phenotypes to NA. The number of genomes with a high
515 quality phenotype for at least one of the 13 drugs was therefore 10,228. Of these 533 were
516 lineage 1, 3581 lineage 2, 805 lineage 3, and 5309 lineage 4. Due to rigorous quality control
517 described above, only samples with high quality phenotypes were tested for each drug,
518 resulting in a range of 6,388-9,418 genomes used in each GWAS.
519
520 **Phylogenetic inference**
521 A pairwise distance matrix was constructed for the full CRyPTIC dataset based on variant
522 calls [79]. For visualisation of the dataset, a neighbour joining tree was built from the
523 distance matrix using the ape package in R and subset to the GWAS dataset. Negative
524 branch lengths were set to zero, and the length was added to the adjacent branch. The
525 branch lengths were square rooted and the tree annotated by lineages assigned by Mykrobe
526 [80].
527
528 **Oligonucleotide/oligopeptide counting**
529 To capture SNP-based variation, indels, and combinations of SNPs and indels, we pursued
530 oligonucleotide and oligopeptide-based approaches, focusing primarily on oligopeptides.
531 Where helpful for clarifying results, we interpreted significant associations using
532 oligonucleotides. Sequence reads were assembled *de novo* using Velvet Optimiser [82] with
533 a starting lower hash value of half the read length, and a higher hash value of the read
534 length minus one; if these were even numbers they were lowered by one. If the total
535 sequence length of the reads in the FASTQ file was greater than $1x10^9$, then the reads were

randomly subsampled prior to assembly down to a sequence length of $1x10^9$ which is around 227x mean coverage. For the oligopeptide analysis, each assembly contig was translated into the six possible reading frames in order to be agnostic to the correct reading frame. 11 amino acid long oligopeptides were counted in a one amino acid sliding window from these translated contigs. 31bp nucleotide oligonucleotides were also counted from the assembled contigs using dsk [83]. For both oligonucleotide and oligopeptide analyses, a unique set of variants across the dataset was created, with the presence or absence of each unique variant determined per genome. An oligonucleotide/oligopeptide was counted as present within a genome if it was present at least once. This resulted in 60,103,864 oligopeptides and 34,669,796 oligonucleotides. Of these, 10,510,261 oligopeptides and 5,530,210 oligonucleotides were variably present in the GWAS dataset of 10,228 genomes.

**Oligonucleotide/oligopeptide alignment**

We used the surrounding context of the contigs that the oligopeptides/oligonucleotides were identified in to assist with their alignment. First, we aligned the contigs of each genome to the H37Rv reference genome [84] using nucmer [85], keeping alignments above 90% identity, assigning a H37Rv position to each base in the contig. Version 3 of the H37Rv strain (NC_000962.3) was used as the reference genome throughout the analysis. All numbering refers to the start positions in the H37Rv version 3 GenBank file. This gave a position for each oligonucleotide identified in the contigs, and after translating the six possible reading frames of the contig, each oligopeptide too. Each oligonucleotide/ oligopeptide was assigned a gene or intergenic region (IR) or both in each genome. These variant/gene combinations were then merged across all genomes into unique variant/gene combinations, where a variant could be assigned to multiple genes or intergenic regions.

Variant/gene combinations were then kept if seen in five or more genomes. In some specific regions where significant oligonucleotides or oligopeptides appeared to be capturing an invariant region, a threshold of just one genome was used to visualise low frequency variants in the region. This was used only for interpretation of the signal in the region, and not for the main analyses. To improve alignment for the most significant genes and intergenic regions, all oligonucleotides/oligopeptides in the gene/IR plus those that aligned to a gene/IR within 1kb were re-aligned to the region using BLAST. Alignments were kept if above 70% identity, recalculated along the whole length of the oligonucleotide/oligopeptide assuming the whole oligonucleotide/oligopeptide aligned. Oligopeptides were aligned to all six possible reading frames and only the correct reading frame was interpreted. An oligonucleotide/oligopeptide was interpreted as unaligned if it did not align to any of the six possible reading frames. A region was determined to be significant if it contained significant oligopeptides above a minor allele frequency (MAF) of 0.1% that were assigned to the region that also aligned using BLAST. If no significant oligopeptides aligned to the correct reading frame of a protein, or if the significant region was intergenic, then oligonucleotides were assessed.

**Covariates**

Isolates were sampled from 9 sites and minimum inhibitory concentrations (MIC) were measured on two versions of the quantitative microtiter plate assays, UKMYC5 and UKMYC6 [31]. UKMYC6 contained adjusted concentrations for some drugs. Therefore in order to account for possible batch effects, we controlled for site plus plate type in the LMM by coding them as binary variables. These plus an intercept were included as covariates in the GWAS analyses.

584

585 **Testing for locus effects**

586 We performed association testing using linear mixed model (LMM) analyses implemented in
587 the software GEMMA to control for population structure [32]. Significance was calculated
588 using likelihood ratio tests. We computed the relatedness matrix from the
589 presence/absence matrix using Java code which calculates the centred relatedness matrix.
590 GEMMA was run using no minor allele frequency cut-off to include all variants. When
591 assessing the most significant regions for each drug, we excluded oligopeptides below 0.1%
592 MAF. To understand the full signal at these regions, oligo-peptides and nucleotides were
593 visualised in alignment figures to interpret the variants captured. When assessing the gene
594 highlighted for each drug, we assessed the LD ($r^2$) of the most significant oligo-peptide or
595 nucleotide in the gene with all other top oligo-peptides or nucleotides for the top 20 genes
596 for the drug. The top variants in the genes noted were not in high LD with known causal
597 variants, in some cases they were in LD with other top 20 gene hits that were less
598 significant.

599

600 **Correcting for multiple testing**

601 Multiple testing was accounted for by applying a Bonferroni correction calculated for each
602 drug. The unit of correction for all studies was the number of unique “phylopatterns”, i.e.
603 the number of unique partitions of individuals according to variant presence/absence for
604 the phenotype tested. An oligopeptide/oligonucleotide was considered to be significant if
605 its $p$-value was smaller than $\alpha/n_p$, where we took $\alpha$ =0.05 to be the genome-wide false
606 positive rate (i.e. family-wide error rate, FWER) and $n_p$ to be the number of unique
607 phylopatterns above 0.1% MAF in the genomes tested for the particular drug. The $-\log_{10}p$

608 significance thresholds for the oligopeptide analyses were: 7.69 (amikacin, kanamycin),
609 7.65 (bedaquiline), 7.64 (clofazimine, levofloxacin), 7.67 (delamanid, ethionamide),
610 7.62 (ethambutol, linezolid), 7.70 (isoniazid), 7.60 (moxifloxacin), 7.71 (rifabutin) and
611 7.68 (rifampicin). The $-\log_{10}p$ significance thresholds for the oligonucleotide analyses were:
612 7.38 (amikacin, kanamycin), 7.34 (bedaquiline, clofazimine, levofloxacin), 7.36 (delamanid,
613 ethionamide), 7.32 (ethambutol), 7.39 (isoniazid, rifabutin), 7.33 (linezolid), 7.31
614 (moxifloxacin) and 7.37 (rifampicin).
615

616 **Estimating sample heritability**

617 Sample heritability is the proportion of the phenotypic variation that can be explained by
618 the bacterial genotype assuming additive effects. This was estimated using the LMM null
619 model in GEMMA [32] from the presence vs. absence matrices for both oligopeptides and
620 oligonucleotides separately. Sample heritability was estimated for the MIC phenotype as
621 well as for the binary sensitive vs. resistant phenotype. The binary phenotypes were
622 determined using the epidemiological cutoff (ECOFF), defined as the MIC that encompasses
623 99% of wild type isolates [31], all those below the ECOFF were considered susceptible, and
624 those above the ECOFF were considered to be resistant.
625

# Acknowledgements

**Acknowledgements – funders**

This work was supported by Wellcome Trust/Newton Fund-MRC Collaborative Award (200205/Z/15/Z); and Bill & Melinda Gates Foundation Trust (OPP1133541). Oxford CRyPTIC consortium members are funded/supported by the National Institute for Health Research (NIHR) Oxford Biomedical Research Centre (BRC), the views expressed are those of the authors and not necessarily those of the NHS, the NIHR or the Department of Health, and the National Institute for Health Research (NIHR) Health Protection Research Unit in Healthcare Associated Infections and Antimicrobial Resistance, a partnership between Public Health England and the University of Oxford, the views expressed are those of the authors and not necessarily those of the NIHR, Public Health England or the Department of Health and Social Care. J.M. is supported by the Wellcome Trust (203919/Z/16/Z). Z.Y. is supported by the National Science and Technology Major Project, China Grant No. 2018ZX10103001. K.M.M. is supported by EMBL's EIPOD3 programme funded by the European Union's Horizon 2020 research and innovation programme under Marie Skłodowska Curie Actions. T.C.R. is funded in part by funding from Unitaid Grant No. 2019-32-FIND MDR. R.S.O. is supported by FAPESP Grant No. 17/16082-7. L.F. received financial support from FAPESP Grant No. 2012/51756-5. B.Z. is supported by the National Natural Science Foundation of China (81991534) and the Beijing Municipal Science & Technology Commission (Z201100005520041). N.T.T.T. is supported by the Wellcome Trust International Intermediate Fellowship (206724/Z/17/Z). G.T. is funded by the Wellcome Trust. R.W. is supported by the South African Medical Research Council. J.C. is supported by

650 the Rhodes Trust and Stanford Medical Scientist Training Program (T32 GM007365). A.L. is
651 supported by the National Institute for Health Research (NIHR) Health Protection Research
652 Unit in Respiratory Infections at Imperial College London. S.G.L. is supported by the Fonds
653 de Recherche en Santé du Québec. C.N. is funded by Wellcome Trust Grant No.
654 203583/Z/16/Z. A.V.R. is supported by Research Foundation Flanders (FWO) under Grant
655 No. G0F8316N (FWO Odysseus). G.M. was supported by the Wellcome Trust (098316,
656 214321/Z/18/Z, and 203135/Z/16/Z), and the South African Research Chairs Initiative of the
657 Department of Science and Technology and National Research Foundation (NRF) of South
658 Africa (Grant No. 64787). The funders had no role in the study design, data collection, data
659 analysis, data interpretation, or writing of this report. The opinions, findings and conclusions
660 expressed in this manuscript reflect those of the authors alone. L.G. was supported by the
661 Wellcome Trust (201470/Z/16/Z), the National Institute of Allergy and Infectious Diseases of
662 the National Institutes of Health under award number 1R01AI146338, the GOSH Charity
663 (VC0921) and the GOSH/ICH Biomedical Research Centre (www.nihr.ac.uk). A.B. is funded
664 by the NDM Prize Studentship from the Oxford Medical Research Council Doctoral Training
665 Partnership and the Nuffield Department of Clinical Medicine. D.J.W. is supported by a Sir
666 Henry Dale Fellowship jointly funded by the Wellcome Trust and the Royal Society (Grant
667 No. 101237/Z/13/B) and by the Robertson Foundation. A.S.W. is an NIHR Senior
668 Investigator. T.M.W. is a Wellcome Trust Clinical Career Development Fellow
669 (214560/Z/18/Z). A.S.L. is supported by the Rhodes Trust. R.J.W. receives funding from the
670 Francis Crick Institute which is supported by Wellcome Trust, (FC0010218), UKRI
671 (FC0010218), and CRUK (FC0010218). T.C. has received grant funding and salary support
672 from US NIH, CDC, USAID and Bill and Melinda Gates Foundation. The computational
673 aspects of this research were supported by the Wellcome Trust Core Award Grant Number

674 203141/Z/16/Z and the NIHR Oxford BRC. Parts of the work were funded by the German
675 Center of Infection Research (DZIF). The Scottish Mycobacteria Reference Laboratory is
676 funded through National Services Scotland. The Wadsworth Center contributions were
677 supported in part by Cooperative Agreement No. U60OE000103 funded by the Centers for
678 Disease Control and Prevention through the Association of Public Health Laboratories and
679 NIH/NIAID grant AI-117312. Additional support for sequencing and analysis was contributed
680 by the Wadsworth Center Applied Genomic Technologies Core Facility and the Wadsworth
681 Center Bioinformatics Core. SYNLAB Holding Germany GmbH for its direct and indirect
682 support of research activities in the Institute of Microbiology and Laboratory Medicine
683 Gauting. N.R. thanks the Programme National de Lutte contre la Tuberculose de
684 Madagascar.
685
686 Computation used the Oxford Biomedical Research Computing (BMRC) facility, a
687 joint development between the Wellcome Centre for Human Genetics and the Big
688 Data Institute supported by Health Data Research UK and the NIHR Oxford
689 Biomedical Research Centre.
690

691 **Competing Interest**

692

693 E.R. is employed by Public Health England and holds an honorary contract with Imperial
694 College London. I.F.L. is Director of the Scottish Mycobacteria Reference Laboratory. S.N.
695 receives funding from German Center for Infection Research, Excellenz Cluster Precision
696 Medicine in Chronic Inflammation, Leibniz Science Campus Evolutionary Medicine of the
697 LUNG (EvoLUNG)tion EXC 2167. P.S. is a consultant at Genoscreen. T.R. is funded by NIH and

DoD and receives salary support from the non-profit organization FIND. T.R. is a co-founder, board member and shareholder of Verus Diagnostics Inc, a company that was founded with the intent of developing diagnostic assays. Verus Diagnostics was not involved in any way with data collection, analysis or publication of the results. T.R. has not received any financial support from Verus Diagnostics. UCSD Conflict of Interest office has reviewed and approved T.R.'s role in Verus Diagnostics Inc. T.R. is a co-inventor of a provisional patent for a TB diagnostic assay (provisional patent #: 63/048.989). T.R. is a co-inventor on a patent associated with the processing of TB sequencing data (European Patent Application No. 14840432.0 & USSN 14/912,918). T.R. has agreed to "donate all present and future interest in and rights to royalties from this patent" to UCSD to ensure that he does not receive any financial benefits from this patent. S.S. is working and holding ESOPs at HaystackAnalytics Pvt. Ltd. (Product: Using whole genome sequencing for drug susceptibility testing for Mycobacterium tuberculosis). G.F.G. is listed as an inventor on patent applications for RBD-dimer-based CoV vaccines. The patents for RBD-dimers as protein subunit vaccines for SARS-CoV-2 have been licensed to Anhui Zhifei Longcom Biopharmaceutical Co. Ltd, China.

**Wellcome Trust Open Access**

This research was funded in part, by the Wellcome Trust/Newton Fund-MRC Collaborative Award [200205/Z/15/Z]. For the purpose of Open Access, the author has applied a CC BY public copyright licence to any Author Accepted Manuscript version arising from this submission.

721 This research was funded, in part, by the Wellcome Trust [214321/Z/18/Z, and
722 203135/Z/16/Z]. For the purpose of open access, the author has applied a CC BY public
723 copyright licence to any Author Accepted Manuscript version arising from this submission.

724

725 **Acknowledgements – people**

726

727 We thank Faisal Masood Khanzada and Alamdar Hussain Rizvi (NTRL, Islamabad, Pakistan),
728 Angela Starks and James Posey (Centers for Disease Control and Prevention, Atlanta, USA),
729 and Juan Carlos Toro and Solomon Ghebremichael (Public Health Agency of Sweden, Solna,
730 Sweden), Iñaki Comas and Álvaro Chiner-Oms (Instituto de Biología Integrativa de Sistemas,
731 Valencia, Spain; CIBER en Epidemiología y Salud Pública, Valencia, Spain; Instituto de
732 Biomedicina de Valencia, IBV-CSIC, Valencia, Spain).

733

734 **Ethics Statement**

735

736 Approval for CRyPTIC study was obtained by Taiwan Centers for Disease Control IRB No.
737 106209, University of KwaZulu Natal Biomedical Research Ethics Committee (UKZN BREC)
738 (reference BE022/13) and University of Liverpool Central University Research Ethics
739 Committees (reference 2286), Institutional Research Ethics Committee (IREC) of The
740 Foundation for Medical Research, Mumbai (Ref nos. FMR/IEC/TB/01a/2015 and
741 FMR/IEC/TB/01b/2015), Institutional Review Board of P.D. Hinduja Hospital and Medical
742 Research Centre, Mumbai (Ref no. 915-15-CR [MRC]), scientific committee of the Adolfo Lutz
743 Institute (CTC-IAL 47-J / 2017) and in the Ethics Committee (CAAE: 81452517.1.0000.0059)

744 and Ethics Committee review by Universidad Peruana Cayetano Heredia (Lima, Peru) and

745 LSHTM (London, UK).

746

**Members of the CRyPTIC consortium (in alphabetical order)**

Correspondence to: Daniel J Wilson (daniel.wilson@bdi.ox.ac.uk)

Sarah G Earle[4], Daniel J Wilson[4], Ivan Barilar[29], Simone Battaglia[1], Emanuele Borroni[1], Angela Pires Brandao[2,3], Alice Brankin[4], Andrea Maurizio Cabibbe[1], Joshua Carter[5], Daniela Maria Cirillo[1], Pauline Claxton[6], David A Clifton[4], Ted Cohen[7], Jorge Coronel[8], Derrick W Crook[4], Viola Dreyer[29], Vincent Escuyer[9], Lucilaine Ferrazoli[3], Philip W Fowler[4], George Fu Gao[10], Jennifer Gardy[11], Saheer Gharbia[12], Kelen Teixeira Ghisi[3], Arash Ghodousi[1,13], Ana Luíza Gibertoni Cruz[4], Louis Grandjean[33], Clara Grazian[14], Ramona Groenheit[44], Jennifer L Guthrie[15,16], Wencong He[10], Harald Hoffmann[17,18], Sarah J Hoosdally[4], Martin Hunt[19,4], Zamin Iqbal[19], Nazir Ahmed Ismail[20], Lisa Jarrett[21], Lavania Joseph[20], Ruwen Jou[22], Priti Kambli[23], Rukhsar Khot[23], Jeff Knaggs[19,4], Anastasia Koch[24], Donna Kohlerschmidt[9], Samaneh Kouchaki[4,25], Alexander S Lachapelle[4], Ajit Lalvani[26], Simon Grandjean Lapierre[27], Ian F Laurenson[6], Brice Letcher[19], Wan-Hsuan Lin[22], Chunfa Liu[10], Dongxin Liu[10], Kerri M Malone[19], Ayan Mandal[28], Mikael Mansjö[44], Daniela Matias[21], Graeme Meintjes[24], Flávia de Freitas Mendes[3], Matthias Merker[29], Marina Mihalic[18], James Millard[30], Paolo Miotto[1], Nerges Mistry[28], David Moore[31,8], Kimberlee A Musser[9], Dumisani Ngcamu[20], Hoang Ngoc Nhung[32], Stefan Niemann[29, 48], Kayzad Soli Nilgiriwala[28], Camus Nimmo[33], Nana Okozi[20], Rosangela Siqueira Oliveira[3], Shaheed Vally Omar[20], Nicholas Paton[34], Timothy EA Peto[4], Juliana Maira Watanabe Pinhata[3], Sara Plesnik[18], Zully M Puyen[35], Marie Sylvianne Rabodoarivelo[36], Niaina Rakotosamimanana[36], Paola MV Rancoita[13], Priti Rathod[21], Esther Robinson[21], Gillian Rodger[4], Camilla Rodrigues[23], Timothy C Rodwell[37,38], Aysha Roohi[4], David Santos-Lazaro[35], Sanchi Shah[28], Thomas Andreas Kohl[29], Grace Smith[21,12], Walter Solano[8], Andrea Spitaleri[1,13], Philip Supply[39], Utkarsha Surve[23], Sabira Tahseen[40], Nguyen Thuy Thuong Thuong[32], Guy Thwaites[32,4], Katharina Todt[18], Alberto Trovato[1], Christian Utpatel[29], Annelies Van Rie[41],

771 Srinivasan Vijay[42], Timothy M Walker[4,32], A Sarah Walker[4], Robin Warren[43], Jim Werngren[44],

772 Maria Wijkander[44], Robert J Wilkinson[45,46,26], Penelope Wintringer[19], Yu-Xin Xiao[22], Yang

773 Yang[4], Zhao Yanlin[10], Shen-Yuan Yao[20], Baoli Zhu[47]

774

775 **Institutions**

776 1 IRCCS San Raffaele Scientific Institute, Milan, Italy

777 2 Oswaldo Cruz Foundation, Rio de Janeiro, Brazil

778 3 Institute Adolfo Lutz, São Paulo, Brazil

779 4 University of Oxford, Oxford, UK

780 5 Stanford University School of Medicine, Stanford, USA

781 6 Scottish Mycobacteria Reference Laboratory, Edinburgh, UK

782 7 Yale School of Public Health, Yale, USA

783 8 Universidad Peruana Cayetano Heredia, Lima, Perú

784 9 Wadsworth Center, New York State Department of Health, Albany, USA

785 10 Chinese Center for Disease Control and Prevention, Beijing, China

786 11 Bill & Melinda Gates Foundation, Seattle, USA

787 12 UK Health Security Agency, London, UK

788 13 Vita-Salute San Raffaele University, Milan, Italy

789 14 University of New South Wales, Sydney, Australia

790 15 The University of British Columbia, Vancouver, Canada

791 16 Public Health Ontario, Toronto, Canada

792 17 SYNLAB Gauting, Munich, Germany

793 18 Institute of Microbiology and Laboratory Medicine, IMLred, WHO-SRL Gauting, Germany

794 19 EMBL-EBI, Hinxton, UK

20 National Institute for Communicable Diseases, Johannesburg, South Africa

21 Public Health England, Birmingham, UK

22 Taiwan Centers for Disease Control, Taipei, Taiwan

23 Hinduja Hospital, Mumbai, India

24 University of Cape Town, Cape Town, South Africa

25 University of Surrey, Guildford, UK

26 Imperial College, London, UK

27 Université de Montréal, Canada

28 The Foundation for Medical Research, Mumbai, India

29 Research Center Borstel, Borstel, Germany

30 Africa Health Research Institute, Durban, South Africa

31 London School of Hygiene and Tropical Medicine, London, UK

32 Oxford University Clinical Research Unit, Ho Chi Minh City, Viet Nam

33 University College London, London, UK

34 National University of Singapore, Singapore

35 Instituto Nacional de Salud, Lima, Perú

36 Institut Pasteur de Madagascar, Antananarivo, Madagascar

37 FIND, Geneva, Switzerland

38 University of California, San Diego, USA

39 Univ. Lille, CNRS, Inserm, CHU Lille, Institut Pasteur de Lille, U1019 - UMR 9017 - CIIL - Center for Infection and Immunity of Lille, F-59000 Lille, France

40 National TB Reference Laboratory, National TB Control Program, Islamabad, Pakistan

41 University of Antwerp, Antwerp, Belgium

42 University of Edinburgh, Edinburgh, UK

819 43 Stellenbosch University, Cape Town, South Africa

820 44 Public Health Agency of Sweden, Solna, Sweden

821 45 Wellcome Centre for Infectious Diseases Research in Africa, Cape Town, South Africa

822 46 Francis Crick Institute, London, UK

823 47 Institute of Microbiology, Chinese Academy of Sciences, Beijing, China

824 48 German Center for Infection Research (DZIF), Hamburg-Lübeck-Borstel-Riems, Germany

# References

1. World Health Organization. Global Tuberculosis Report. ; 2020.
2. Shah NS, Auld SC, Brust JCM, Mathema B, Ismail N, Moodley P, et al. Transmission of Extensively Drug-Resistant Tuberculosis in South Africa. N Engl J Med. 2017; 376(3): 243-253.
3. World Health Organization. WHO Consolidated Guidelines on Tuberculosis, Module 4: Treatment - Drug-Resistant Tuberculosis Treatment. ; 2020.
4. World Health Organization. Rapid Communication: Key changes to the treatment of drug-resistant tuberculosis. ; 2019.
5. Kranzer K, Kalsdorf B, Heyckendorf J, Andres S, Merker M, Hofmann-Thiel S, et al. New World Health Organization Treatment Recommendations for Multidrug-Resistant Tuberculosis: Are We Well Enough Prepared? Am J Respir Crit Care Med. 2019; 200(4).
6. Andres S, Merker M, Heyckendorf J, Kalsdorf B, Rumetshofer R, Indra A, et al. Bedaquiline-Resistant Tuberculosis: Dark Clouds on the Horizon. Am J Respir Crit Care Med. 2020; 201(12).
7. Polsfuss S, Hofmann-Thiel S, Merker M, Krieger D, Niemann S, Rüssmann H, et al. Emergence of Low-level Delamanid and Bedaquiline Resistance During Extremely Drug-resistant Tuberculosis Treatment. Clin Infect Dis. 2019; 69(7): 1229-1231.
8. Islam M, Hameed H, Mugweru J, Chhotaray C, Wang C, Tan Y, et al. Drug resistance mechanisms and novel drug targets for tuberculosis therapy. J Genet Genomics. 2016; 44(1): 21-37.
9. Goossens S, Sampson S, Van Rie A. Mechanisms of Drug-Induced Tolerance in Mycobacterium tuberculosis. Clin Microbiol Rev. 2020; 34(1): e00141-20.

10. Pankhurst L, Del Ojo Elias C, Votintseva A, Walker T, Cole K, Davies J, et al. Rapid, comprehensive, and affordable mycobacterial diagnosis with whole-genome sequencing: a prospective study. Lancet Respir Med. 2016; 4(1): 49-58.

11. The CRyPTIC Consortium and the 100,000 Genomes Project. Prediction of Susceptibility to First-Line Tuberculosis Drugs by DNA Sequencing. N Engl J Med. 2018; 379(15): 1403-1415.

12. Walker TM, Gibertoni Cruz AL, Tim E. P, Smith EG, Esmail H, Crook DW. Tuberculosis is changing. Lancet Infec Dis. 2017; 17(4): 359-361.

13. Makhado NA, Matabane E, Faccin M, Pinçon C, Jouet A, Boutachkourt F, et al. Lancet Infect Dis. Outbreak of multidrug-resistant tuberculosis in South Africa undetected by WHO-endorsed commercial tests: an observational study. 2018; 18(12): 1350-1359.

14. Boehme CC, Nabeta P, Hillemann D, Nicol MP, Shenai S, Krapp F, et al. Rapid Molecular Detection of Tuberculosis and Rifampin Resistance. N Engl J Med. 2010; 363(11): 1005-1015.

15. Boehme C, Nicol M, Nabeta P, Michael J, Gotuzzo E, Tahirli R, et al. Feasibility, diagnostic accuracy, and effectiveness of decentralised use of the Xpert MTB/RIF test for diagnosis of tuberculosis and multidrug resistance: a multicentre implementation study. Lancet. 2011; 377(9776): 1495-1505.

16. Sanchez-Padilla E, Merker M, Beckert P, Jochims F, Dlamini T, Kahn P, et al. Detection of Drug-Resistant Tuberculosis by Xpert MTB/RIF in Swaziland. N Engl J Med. 2015; 372(12): 1181-1182.

17. Miotto P, Tessema B, Tagliani E, Chindelevitch L, Starks AM, Emerson C, et al. A standardised method for interpreting the association between mutations and phenotypic drug resistance in Mycobacterium tuberculosis. Eur Respir J. 2017; 50(6): 1701354.

18. Farhat MR, Shapiro BJ, Kieser KJ, Sultana R, Jacobson KR, Victor TC, et al. Genomic analysis identifies targets of convergent positive selection in drug-resistant Mycobacterium tuberculosis. Nat Genet. 2013; 45(10): 1183-1189.

19. Zhang H, Li D, Zhao L, Fleming J, Lin NWT, Liu Z, et al. Genome sequencing of 161 Mycobacterium tuberculosis isolates from China identifies genes and intergenic regions associated with drug resistance. Nat Genet. 2013; 45(10): 1255-1260.

20. Earle SG, Wu Ch, Charlesworth J, Stoesser N, Gordon NC, Walker TM, et al. Identifying lineage effects when controlling for population structure improves power in bacterial association studies. Nat Microbiol. 2016; 1(5): 16041.

21. Nair MB, Mallard K, Ali S, Abdallah AM, Alghamdi S, Alsomali M, et al. Genome-wide analysis of multi- and extensively drug-resistant Mycobacterium tuberculosis. Nat Genet. 2018; 50(2): 307-316.

22. Farhat M, Freschi L, Calderon R, Ioerger T, Snyder M, Meehan C, et al. GWAS for quantitative resistance phenotypes in Mycobacterium tuberculosis reveals resistance genes and regulatory regions. Nat Commun. 2019; 10(2128).

23. Oppong YEA, Phelan J, Perdigão J, Machado D, Miranda A, Portugal I, et al. Genome-wide analysis of Mycobacterium tuberculosis polymorphisms reveals lineage-specific associations with drug resistance. BMC Genomics. 2019; 20(1): 252.

24. Farhat M, Sultana R, Iartchouk O, Bozeman S, Galagan J, Sisk P, et al. Genetic Determinants of Drug Resistance in Mycobacterium tuberculosis and Their Diagnostic Value. Am J Respir Crit Care Med. 2016; 194(5): 621-630.

25. Walker TM, Kohl TA, Omar SV, Hedge J, Del Ojo Elias C, Bradley P, et al. Whole-genome sequencing for prediction of Mycobacterium tuberculosis drug susceptibility and resistance: A retrospective cohort study. The Lancet Infectious Diseases. 2015; 15(10): 1193-1202.

26. Price AL, Zaitlen NA, Reich D, Patterson N. New approaches to population stratification in genome-wide association studies. Nat Rev Genet. 2010; 11(7): 459-463.

27. World Health Organization. Technical report on critical concentrations for TB drug susceptibility testing of medicines used in the treatment of drug-resistant TB. ; 2018.

28. Schön T, Miotto P, Köser CU, Viveiros M, Böttger E, Cambau E. Mycobacterium tuberculosis drug-resistance testing: challenges, recent developments and perspectives. Clin Microbiol Infect. 2017; 23(3): 154-160.

29. Sreevatsan S, Stockbauer KE, Pan X, Kreiswirth BN:MSL, Jacobs WR, Jr TA, et al. Ethambutol resistance in Mycobacterium tuberculosis: critical role of embB mutations. Antimicrob Agents Chemother. 1997; 41(8): 1677-1681.

30. Rancoita P, Cugnata F, Gibertoni Cruz A, Borroni E, Hoosdally S, Walker T, et al. Validating a 14-Drug Microtiter Plate Containing Bedaquiline and Delamanid for Large-Scale Research Susceptibility Testing of Mycobacterium tuberculosis. Antimicrob Agents Chemother. 2018; 62(9): e00344-18.

31. The CRyPTIC Consortium. Epidemiological cutoff values for a 96-well broth microdilution plate for high-throughput research antibiotic susceptibility testing of M. tuberculosis. medRxiv doi:101101/2021022421252386. 2021.

32. Zhou X, Stephens M. Genome-wide efficient mixed-model analysis for association studies. Nat Genet. 2012; 44(7): 821-824.

33. Pantel A, Petrella S, Veziris N, Brossier F, Bastian S, Jarlier V, et al. Extending the definition of the GyrB quinolone resistance-determining region in Mycobacterium tuberculosis DNA gyrase for assessing fluoroquinolone resistance in M. tuberculosis. Antimicrob Agents Chemother. 2012; 56(4): 1990-1996.

34. Blower TR, Williamson BH, Kerns RJ, Berger JM. Structure of tuberculosis quinolone–gyrase complex. Proc Natl Acad Sci USA. 2016; 113(7): 1706-1713.

35. Sharma G, Upadhyay S, Srilalitha M, Nandicoori V, Khosla S. The interaction of mycobacterial protein Rv2966c with host chromatin is mediated through non-CpG methylation and histone H3/H4 binding. Nucleic Acids Res. 2015; 43(8): 3922-3937.

36. Lai YP, Ioerger T. Exploiting Homoplasy in Genome-Wide Association Studies to Enhance Identification of Antibiotic-Resistance Mutations in Bacterial Genomes. Evol Bioinform Online. 2020.

37. Dixit, A.; Freschi, L.; Vargas, R.; Calderon, R; Sacchettini, J; Drobniewski, F; Galea, J.T.; Contreras, C; Yataco, R; Zhang, Z; Lecca, L; Kolokotronis, S-O; Mathema, B; Farhat, M.R. Whole genome sequencing identifies bacterial factors affecting transmission of multidrug-resistant tuberculosis in a high-prevalence setting. Sci Rep. 2019; 9(5602).

38. Kumar N, Radhakrishnan A, Wright C, Chou T, Lei H, Bolla J, et al. Crystal structure of the transcriptional regulator Rv1219c of Mycobacterium tuberculosis. Protein Sci. 2014; 23(4): 423-432.

39. Wang K, Pei H, Huang B, Zhu X, Zhang J, Zhou B, et al. The expression of ABC efflux pump, Rv1217c-Rv1218c, and its association with multidrug resistance of Mycobacterium tuberculosis in China. Curr Microbiol. 2013; 66(3): 222-226.

40. Chakhaiyar P, Nagalakshmi Y, Aruna B, Murthy K, Katoch V, Hasnain S. Regions of high antigenicity within the hypothetical PPE major polymorphic tandem repeat open-reading frame, Rv2608, show a differential humoral response and a low T cell response in various categories of patients with tuberculosis. J Infect Dis. 2004; 190(7): 1237-1244.

41. Coler R, Day T, Ellis R, Piazza F, Beckmann A, Vergara J, et al. The TLR-4 agonist adjuvant, GLA-SE, improves magnitude and quality of immune responses elicited by the ID93 tuberculosis vaccine: first-in-human trial. NPJ Vaccines. 2018; 3(34).

42. Bhattacharyya K, Nemaysh V, Joon M, Pratap R, Varma-Basil M, M. B, et al. Correlation of drug resistance with single nucleotide variations through genome analysis and experimental validation in a multi-drug resistant clinical isolate of M. tuberculosis. BMC Microbiol. 2020; 20(223).

43. Burian J, Ramón-García S, Sweet G, Gómez-Velasco A, Av-Gay Y, Thompson C. The mycobacterial transcriptional regulator whiB7 gene links redox homeostasis and intrinsic antibiotic resistance. J Biol Chem. 2012; 287(1): 299-310.

44. Ramón-García S, Ng C, Jensen P, Dosanjh M, Burian J, Morris R, et al. WhiB7, an Fe-S-dependent transcription factor that activates species-specific repertoires of drug resistance determinants in actinobacteria. J Biol Chem. 2013; 288(48): 34514-34528.

45. Morris R, Nguyen L, Gatfield J, Visconti K, Nguyen K, Schnappinger D, et al. Ancestral antibiotic resistance in Mycobacterium tuberculosis. Proc Natl Acad Sci U S A. 2005; 102(34): 12200-12205.

46. Reeves A, Campbell P, Sultana R, Malik S, Murray M, Plikaytis B, et al. Aminoglycoside cross-resistance in Mycobacterium tuberculosis due to mutations in the 5' untranslated region of whiB7. ntimicrob Agents Chemother. 2013; 57(4): 1857-1865.

47. Hicks N, Carey A, Yang J, Zhao Y, Fortune S. Bacterial Genome-Wide Association Identifies Novel Factors That Contribute to Ethionamide and Prothionamide Susceptibility in Mycobacterium tuberculosis. mBio. 2019; 10(2): e00616-19.

48. Maus C, Plikaytis B, Shinnick T. Mutation of tlyA Confers Capreomycin Resistance in Mycobacterium tuberculosis. Antimicrob Agents Chemother. 2005; 49(2): 571-577.

49. Johansen S, Maus C, Plikaytis B, Douthwaite S. Capreomycin Binds across the Ribosomal Subunit Interface Using tlyA-Encoded 2'-O-Methylations in 16S and 23S rRNAs. Mol Cell. 2006; 23(2): 173-182.

50. Arenas NE, Salazar LM, Soto CY, Vizcaíno C, Patarroyo ME, Patarroyo MA, et al. Molecular modeling and in silico characterization of Mycobacterium tuberculosis TlyA: Possible misannotation of this tubercle bacilli-hemolysin. BMC Struct Biol. 2011; 11(16).

51. Monshupanee T, Johansen SK, Dahlberg AE, Douthwaite S. Capreomycin susceptibility is increased by TlyA-directed 2'-O-methylation on both ribosomal subunits. Mol Microbiol. 2012; 85: 1194-1203.

52. Zhao J, Wei W, Yan H, Zhou Y, Li Z, Chen Y, et al. Assessing capreomycin resistance on tlyA deficient and point mutation (G695A) Mycobacterium tuberculosis strains using multi-omics analysis. Int J Med Microbiol. 2019; 309(7).

53. Meza AN, Cambui CCN, Moreno ACR, Fessel MR, Balan A. Mycobacterium tuberculosis CysA2 is a dual sulfurtransferase with activity against thiosulfate and 3-mercaptopyruvate and interacts with mammalian cells. Sci Rep. 2019; 9(16791).

54. Cipollone R, Ascenzi P, Visca P. Common themes and variations in the rhodanese superfamily. IUBMB Life. 2007; 59: 51-59.

55. Phong T, Ha do T, Volker U, Hammer E. Using a Label Free Quantitative Proteomics Approach to Identify Changes in Protein Abundance in Multidrug-Resistant Mycobacterium tuberculosis. Indian J Microbiol. 2015; 55(2): 219-230.

56. Sassetti CM, Boyd DH, Rubin EJ. Genes required for mycobacterial growth defined by high density mutagenesis. Mol Microbiol. 2003; 48: 77-84.

57. Driscoll M, McLean K, Levy C, Mast N, Pikuleva I, Lafite P, et al. Structural and biochemical characterization of Mycobacterium tuberculosis CYP142: evidence for multiple cholesterol 27-hydroxylase activities in a human pathogen. J Biol Chem. 2010; 285(49): 38270-38282.

58. García-Fernández E, Frank D, Galán B, Kells P, Podust L, García J, et al. A highly conserved mycobacterial cholesterol catabolic pathway. Environ Microbiol. 2013; 15(8): 2342-2359.

59. Ortiz de Montellano P. Potential drug targets in the Mycobacterium tuberculosis cytochrome P450 system. J Inorg Biochem. 2018; 180(235-245).

60. Ouellet H, Lang J, Couture M, Ortiz de Montellano P. Reaction of Mycobacterium tuberculosis cytochrome P450 enzymes with nitric oxide. Biochemistry. 2009; 48(5): 863-872.

61. Yano T, Kassovska-Bratinova S, Teh J, Winkler J, Sullivan K, Isaacs A, et al. Reduction of clofazimine by mycobacterial type 2 NADH:quinone oxidoreductase: a pathway for the generation of bactericidal levels of reactive oxygen species. J Biol Chem. 2011; 286(12): 10276-10287.

62. Molle V, Kremer L, Girard-Blanc C, Besra G, Cozzone A, Prost JF. An FHA Phosphoprotein Recognition Domain Mediates Protein EmbR Phosphorylation by PknH, a Ser/Thr Protein Kinase from Mycobacterium tuberculosis. Biochemistry. 2003; 42(51): 15300-15309.

63. Sharma K, Gupta M, Pathak M, Gupta N, Koul A, Sarangi S, et al. Transcriptional control of the mycobacterial embCAB operon by PknH through a regulatory protein, EmbR, in vivo. J Bacteriol. 2006; 188(8): 2936-2944.

64. Sreevatsan S, Stockbauer K, Pan X, Kreiswirth B, Moghazeh S, Jacobs WJ, et al. Ethambutol resistance in Mycobacterium tuberculosis: critical role of embB mutations. Antimicrob Agents Chemother. 1997; 41(8): 1677-1681.

65. Cavazos A, Prigozhin DM, Alber T. Structure of the Sensor Domain of Mycobacterium tuberculosis PknH Receptor Kinase Reveals a Conserved Binding Cleft. J Mol Biol. 2012; 422(4): 488-494.

66. Papavinasasundaram KG, Chan B, Chung JH, Colston MJ, Davis EO, Av-Gay Y. Deletion of the Mycobacterium tuberculosis pknH Gene Confers a Higher Bacillary Load during the Chronic Phase of Infection in BALB/c Mice. J Bacteriol. 2005; 187(16): 5751-5760.

67. Deep A, Kaundal S, Agarwal S, Singh R, Thakur KG. Crystal structure of Mycobacterium tuberculosis VapC20 toxin and its interactions with cognate antitoxin, VapB20, suggest a model for toxin–antitoxin assembly. FEBS J. 2017; 284: 4066-4082.

68. Winther K, Brodersen D, Brown A, Gerdes K. VapC20 of Mycobacterium tuberculosis cleaves the Sarcin–Ricin loop of 23S rRNA. Nat Commun. 2013; 4(2796).

69. Colangeli R, Jedrey H, Kim S, Connell R, Ma S, Chippada Venkata UD, et al. Bacterial Factors That Predict Relapse after Tuberculosis Therapy. N Engl J Med. 2018; 379(9): 823-833.

70. Walsh KF, Vilbrun SC, Souroutzidis A, Delva S, Joissaint G, Mathurin L, et al. Improved Outcomes With High-dose Isoniazid in Multidrug-resistant Tuberculosis Treatment in Haiti. Clin Infect Dis. 2019; 69(4): 717-719.

71. Dooley KE, Miyahara S, von Groote-Bidlingmaier F, Sun X, Hafner R, Rosenkranz SL, et al. Early Bactericidal Activity of Different Isoniazid Doses for Drug-Resistant Tuberculosis (INHindsight): A Randomized, Open-Label Clinical Trial. Am J Respir Crit Care Med. 2020; 201(11).

72. Decroo T, de Jong BC, Piubello A, Souleymane MB, Lynen L, Van Deun A. High-Dose First-Line Treatment Regimen for Recurrent Rifampicin-Susceptible Tuberculosis. Am J Respir Crit Care Med. 2020; 201(12).

73. van Ingen J, Aarnoutse R, de Vries G, Boeree M, van Soolingen D. Low-level rifampicin-resistant Mycobacterium tuberculosis strains raise a new therapeutic challenge. Int J Tuberc Lung Dis. 2011; 15(7): 990-992.

74. Sirgel FA, Warren RM, Böttger EC, Klopper M, Victor TC, van Helden PD. The Rationale for Using Rifabutin in the Treatment of MDR and XDR Tuberculosis Outbreaks. PLoS One. 2013; 8(3): e59414.

75. Farhat MR, Jacobson KR, Franke MF, Kaur D, Sloutsky A, Mitnick CD, et al. Gyrase Mutations Are Associated with Variable Levels of Fluoroquinolone Resistance in Mycobacterium tuberculosis. J Clin Microbiol. 2016; 54(3).

76. Disratthakit A, Prammananan T, Tribuddharat C, Thaipisuttikul I, Doi N, Leechawengwongs M, et al. Role of gyrB Mutations in Pre-extensively and Extensively Drug-Resistant Tuberculosis in Thai Clinical Isolates. Antimicrob Agents Chemother. 2016; 60(9): 5189–5197.

77. Malik S, Willby M, Sikes D, Tsodikov OV, & Posey JE. New insights into fluoroquinolone resistance in Mycobacterium tuberculosis: functional genetic analysis of gyrA and gyrB mutations. PloS one. 2012; 7(6): e39754.

78. World Health Organization. Catalogue of mutations in Mycobacterium tuberculosis complex and their association with drug resistance. ; 2021. Report No.: ISBN: 9789240028173.

79. The CRyPTIC Consortium. A data compendium of M. tuberculosis antibiotic resistance. In prep. .

80. Bradley P, Gordon NC, Walker TM, Dunn L, Heys S, Huang B, et al. Rapid antibiotic-resistance predictions from genome sequence data for Staphylococcus aureus and Mycobacterium tuberculosis. Nature Communications. 2015; 6: 10063.

81. Hunt MH, Letcher B, Malone K, Nguyen G, Hall MB, Colquhoun RM, et al. Minos: graph adjudication and joint genotyping of cohorts of bacterial genomes. In prep. .

82. Zerbino DR, Birney E. Velvet: algorithms for de novo short read assembly using de Bruijn graphs. Genome research. 2008; 18(5): 821-829.

83. Rizk G, Lavenier D, Chikhi R. DSK: k-mer counting with very low memory usage. Bioinformatics. 2013; 29(5): 652-653.

84. Cole S, Brosch R, Parkhill J, Garnier T, Churcher C, Harris D, et al. Deciphering the biology of Mycobacterium tuberculosis from the complete genome sequence. Nature. 1998; 393(6685): 537-544.

85. Kurtz S, Phillippy A, Delcher A, Smoot M, Shumway M, Antonescu C, et al. Versatile and open software for comparing large genomes. Genome Biol. 2004; 5(2): R12.